Acta Crystallographica Section D
Biological Crystallography
ISSN 0907-4449

Structure of a compact conformation of linear diubiquitin

Ahmed Rohaim,[a,b,c] Masato Kawasaki,[a,b] Ryuichi Kato,[a,b] Ivan Dikic[d] and Soichi Wakatsuki[a,b]*

[a]Structural Biology Research Center, Photon Factory, Institute of Materials Structure Science, High Energy Accelerator Research Organization (KEK), Tsukuba, Ibaraki 305-0801, Japan, [b]Graduate University for Advanced Studies, Hayama, Kanagawa 240-0193, Japan, [c]Department of Biophysics, Faculty of Science, Cairo University, Giza, Egypt, and [d]Institute of Biochemistry II, Goethe University School of Medicine, Frankfurt (Main), Germany

Correspondence e-mail: soichi.wakatsuki@kek.jp

Received 11 October 2011
Accepted 28 November 2011

PDB Reference: diubiquitin, 3axc.

Post-translational modifications involving ubiquitin regulate a wide range of biological processes including protein degradation, responses to DNA damage and immune signalling. Ubiquitin polymerizes into chains which may contain eight different linkage types; the ubiquitin C-terminal glycine can link to one of the seven lysine residues or the N-terminal amino group of methionine in the distal ubiquitin molecule. The latter head-to-tail linkage type, referred to as a linear ubiquitin chain, is involved in NF-κB activation through specific interactions with NF-κB essential modulator (NEMO). Here, a crystal structure of linear diubiquitin at a resolution of 2.2 Å is reported. Although the two ubiquitin moieties do not interact with each other directly, the overall structure adopts a compact but not completely closed conformation with a few intermoiety contacts. This structure differs from the previously reported extended conformation, which resembles Lys63-linked diubiquitin, suggesting that the linear polyubiquitin chain is intrinsically flexible and can adopt multiple conformations.

1. Introduction

Ubiquitination is an important type of protein post-translational modification (Hershko & Ciechanover, 1998; Pickart, 2001). Ubiquitin acts as a cellular signal involved in numerous signalling pathways that are dynamically controlled in a spatial and temporal manner, thus contributing to the regulation of gene transcription, proteasome-dependent protein degradation, DNA repair, cell-cycle regulation, inflammation and immune responses (reviewed in Grabbe *et al.*, 2011). Unlike other post-translational modifications, such as phosphorylation and methylation, ubiquitin signalling can be diversified *via* the formation of distinct ubiquitin chains (Hershko & Ciechanover, 1998; Ikeda & Dikic, 2008; Winget & Mayor, 2010). Ubiquitination involves a cascade of enzymatic reactions orchestrated by three classes of enzymes, E1, E2 and E3, with E2 determining the type of chain linkage and E3 accounting for substrate specificity (Hershko & Ciechanover, 1998; Pickart, 2001). Notably, ubiquitin itself is a target protein *via* seven lysine residues (Lys6, Lys11, Lys27, Lys29, Lys33, Lys48 and Lys63), which can function as attachment sites for another ubiquitin molecule; this results in structurally diverse polyubiquitin chains that differentially contribute to intracellular signalling (Ikeda & Dikic, 2008; Li & Ye, 2008). All seven residues have been shown to be involved in chain formation *in vivo* (Xu & Peng, 2006). Linear polyubiquitin chains are characterized by head-to-tail ubiquitin moieties, *i.e.* the C-terminus of one ubiquitin (distal) is covalently attached *via* a normal peptide bond to the N-terminus of another

ubiquitin (proximal; Iwai & Tokunaga, 2009). This reaction is catalyzed by a linear ubiquitin chain-assembly complex (LUBAC) composed of three subunits, HOIP, HOIL-1 and SHARPIN, that catalyze linear ubiquitination of NEMO *in vivo*, resulting in activation of the NF-κB pathway (Kirisako *et al.*, 2006; Tokunaga *et al.*, 2009, 2011; Ikeda *et al.*, 2011; Gerlach *et al.*, 2011).

Different linkage types and potentially the lengths of the ubiquitin chains have been proposed to regulate specificity in ubiquitin signalling networks (Ikeda *et al.*, 2010). For instance, monoubiquitination mediates membrane transport and endocytosis of cell-surface receptors (Hicke, 2001; Haglund *et al.*, 2003). Lys48- and Lys63-linked ubiquitin chains have been extensively studied for more than two decades; the former targets proteins for proteasomal degradation, whereas the latter contributes to multiple proteasome-independent signalling processes (Ikeda & Dikic, 2008; Li & Ye, 2008). The distinct signalling properties of various ubiquitin chains originate from structural differences among the modifications, which are detected by specialized ubiquitin-binding domains (Dikic *et al.*, 2009). For example, linear polyubiquitin chains activate the NF-κB pathway *via* selective noncovalent binding to the UBAN (ubiquitin binding in ABIN and NEMO) domain of NEMO (Rahighi *et al.*, 2009). Although the linear ubiquitin chain was thought to mimic the Lys63-linked chain owing to the proximity of Lys63 and the N-terminus, a recent study showed that the NEMO UBAN domain distinguishes linear chains from Lys63-linked chains (Rahighi *et al.*, 2009).

Free polyubiquitin chains assume different conformations depending on the linkage type. Crystal and nuclear magnetic resonance (NMR) structures of Lys48-linked chains revealed a closed conformation, a result of intermoiety interactions among Ile44-containing hydrophobic patches (Cook *et al.*, 1992; Eddins *et al.*, 2007). In contrast, both Lys63-linked and linear chains assume an extended conformation that lacks intermoiety interactions (Komander *et al.*, 2009). Interestingly, another group showed that Lys63-linked tetraubiquitin adopts an extended conformation in the crystal structure, while an SAXS analysis revealed that it adopts an ensemble of conformations that are more compact in solution (Datta *et al.*, 2009). A recent study revealed that the conformations of crystallized Lys11- and Lys6-linked diubiquitins differed from those of Lys48- and Lys63-linked diubiquitins (Bremm *et al.*, 2010; Matsumoto *et al.*, 2010; Virdee *et al.*, 2010). These observations may reflect linkage-mediated structural differences in the polyubiquitin chains. Here, we describe a compact crystal structure of linear diubiquitin that differs from the previously reported structure.

2. Materials and methods

2.1. Protein expression and purification

GST-tagged linear diubiquitin was expressed in *Escherichia coli* BL21 (DE3) as described previously (Rahighi *et al.*, 2009). A culture containing 40 ml LB bacterial solution was transferred to a larger culture containing 4 l LB medium. At an OD_{600} of 0.6, expression was induced with 300 µ*M* isopropyl β-D-1-thiogalactopyranoside and the culture was continued at 298 K for 16 h. After bacteria had been harvested at 7000*g* for 10 min, pellets were frozen at 193 K for 12 h and resuspended in lysis buffer (50 m*M* Tris–HCl pH 8.0, 100 m*M* NaCl with protease inhibitors from Roche). Cells were ruptured using sonication and whole-cell lysates were centrifuged at 40 000*g* for 30 min. The supernatant was added to Glutathione Sepharose 4B resin (GE Healthcare) and incubated at 277 K for 8 h. The resin mixture was washed (12 times the bed volume) with PBS buffer (100 m*M* NaCl, 2 m*M* KCl, 10 m*M* Na_2HPO_4, 1.7 m*M* KH_2HPO_4 pH 7.4) and then incubated with 50 units of thrombin protease (GE Healthcare) for 6 h at 295 K to cleave the GST tag. The cleaved protein was subjected to size-exclusion chromatography using a HiLoad 26/60 Superdex 75 column (GE Healthcare). The protein sample was concentrated to 28 mg ml^{-1} using an Amicon ultracentrifuge tube (10 kDa cutoff).

Table 1
Data-collection and refinement statistics for linear diubiquitin.

Values in parentheses are for the highest resolution shell.

Space group	*P*1
Unit-cell parameters (Å, °)	a = 33.26, b = 35.31, c = 35.84, α = 91.79, β = 112.85, γ = 112.88
Wavelength (Å)	1.0000
Resolution (Å)	50–2.2 (2.24–2.20)
$R_{\rm merge}$† (%)	4.9 (12.8)
$\langle I/\sigma(I)\rangle$	58.6 (19.6)
Completeness (%)	97.9 (96.1)
Multiplicity	7.5 (7.2)
$R_{\rm work}/R_{\rm free}$‡ (%)	20.6/27.8
Total No. of reflections	51360
No. of unique reflections	6959
No. of atoms	
Protein atoms	1183
Water molecules	35
B factors (Å^2)	
Protein (average)	22.9
Water	20.9
R.m.s. deviations	
Bond lengths (Å)	0.013
Bond angles (°)	1.509

† $R_{\rm merge} = \sum_{hkl}\sum_i |I_i(hkl) - \langle I(hkl)\rangle| / \sum_{hkl}\sum_i I_i(hkl)$, where $I_i(hkl)$ is the intensity of the ith measurement of reflection hkl and $\langle I(hkl)\rangle$ is the mean value of $I_i(hkl)$ for all i measurements. ‡ $R = \sum_{hkl} \big||F_{\rm obs}| - |F_{\rm calc}|\big| / \sum_{hkl} |F_{\rm obs}|$, where $F_{\rm obs}$ is the observed structure factor and $F_{\rm calc}$ is the calculated structure factor. $R_{\rm free}$ was calculated for a randomly chosen 5% of the reflections; $R_{\rm work}$ was calculated from the remaining 95% of the reflections.

2.2. Crystallization and structure determination

The concentrated protein sample was crystallized using commercially available crystallization kits from Hampton Research (Crystal Screen, Crystal Screen 2, PEG/Ion, PEG/Ion 2 and Index) and Emerald BioSystems (Wizard I and II). Protein crystallization was screened in 576 conditions using an automated crystallization robot (Hiraki *et al.*, 2006) and the best crystal was obtained using Crystal Screen condition No. 6, which consisted of 0.2 *M* magnesium chloride hexahydrate, 0.1 *M* Tris–HCl pH 8.5, 30%(*w*/*v*) polyethylene glycol 4000; however, the initial X-ray diffraction was poor owing to the presence of multiple crystals. The best diffraction results were

obtained after optimizing the conditions using 30% PEG 4000, 0.1 *M* Tris–HCl, 0.1 *M* $MgCl_2$, 30% dioxane, 30% 2-propanol at pH 7.5. Crystals grew in 3–5 d, after which they were flash-cooled at 95 K under a nitrogen-gas flow using glycerol (final concentration 12%) as a cryoprotectant. The crystal diffracted to 2.2 Å resolution. X-ray diffraction experiments were carried out on beamline BL-5A of the Photon Factory and data were processed and scaled using *HKL*-2000 (Otwinowski & Minor, 1997). We used the *CCP*4 suite (Winn *et al.*, 2011) to solve the structure with *MOLREP* (Vagin & Teplyakov, 2010) using ubiquitin as the search model (PDB entry 1ubq; Vijay-Kumar *et al.*, 1987); the structure was initially refined using several cycles of *REFMAC*5 (Murshudov *et al.*, 2011). Model building and structure refinement were performed using *Coot* (Emsley *et al.*, 2010). The crystal structure contained one monomer (one diubiquitin chain) in the asymmetric unit. The initial model matched the electron-density map well except for the linker region, which was less well defined but improved after several cycles of refinement and became visible at σ = 1.0. Final data-collection and refinement statistics are summarized in Table 1.

3. Results and discussion

3.1. Crystal structure of linear diubiquitin

Linear diubiquitin was crystallized in space group *P*1, with one molecule in the asymmetric unit. The structure of linear diubiquitin observed in this study is compact and distinct from the previously reported open conformation (Komander *et al.*, 2009; Fig. 1). The two ubiquitin moieties are arranged with opposite orientations (Fig. 1). Although the overall structure is compact, it is not closed. The linker region between the two ubiquitin moieties exhibits a high degree of flexibility, as indicated by its high temperature factors (Table 2). Additionally, elevated temperature factors are also observed for residues Gln31–Gly35 of the proximal ubiquitin (C-terminal moiety), which are located in the C-terminal portion of the α-helix which faces the distal ubiquitin (N-terminal moiety). At the interface between the two ubiquitin moieties, the side-chain carboxylate of Glu51 in the distal ubiquitin faces the main-chain carbonyl groups of Asp32 and Lys33 in the proximal ubiquitin, despite their electrostatic repulsion. These observations suggest that the compact conformation is not

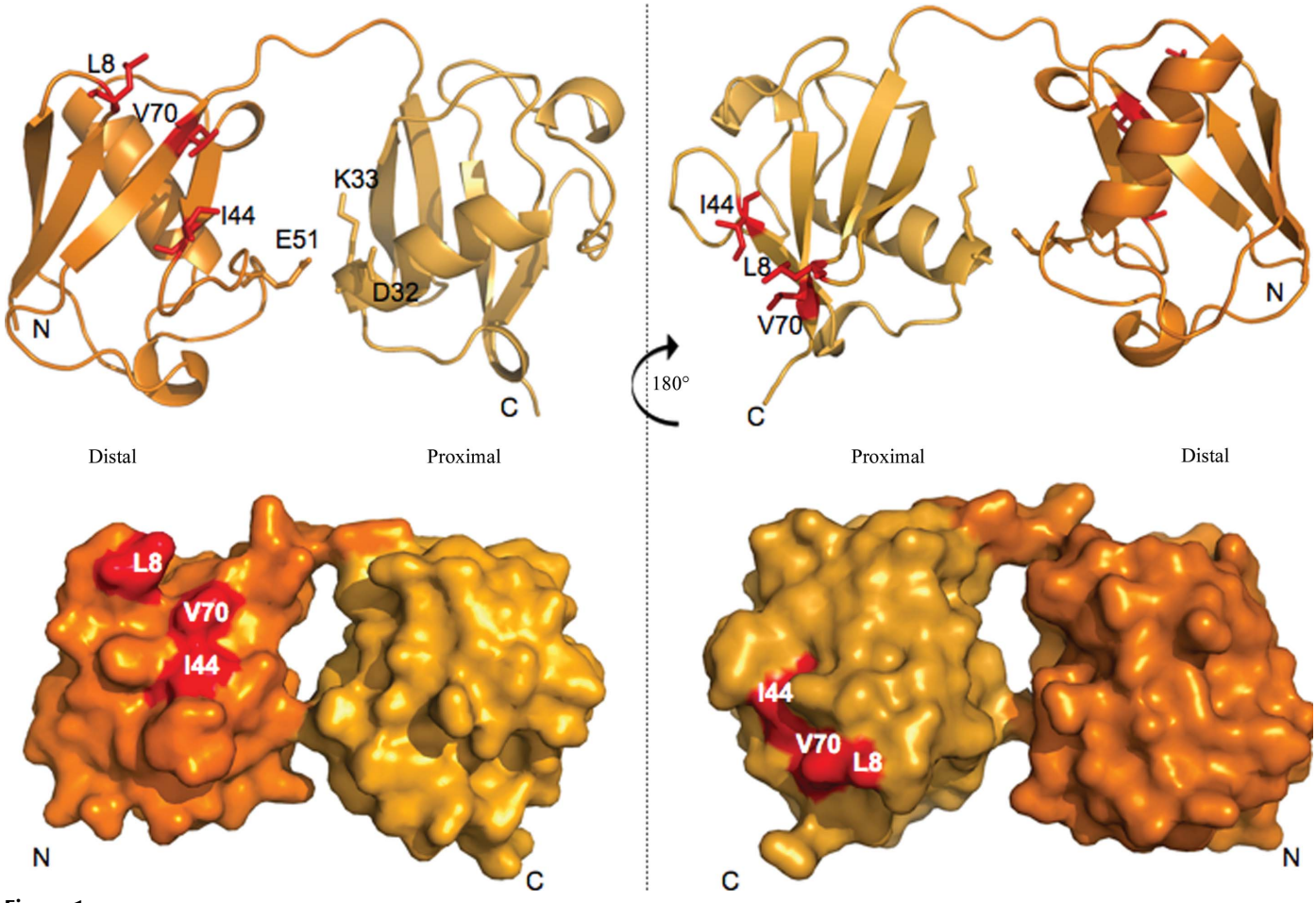

Figure 1
Top, ribbon representation of the crystal structure of linear diubiquitin. The two views are related by a 180° rotation around the vertical axis. The overall conformation is relatively compact. The two ubiquitin subunits have the same secondary structure, including a five-stranded β-sheet, a 3.5-turn α-helix and a short 3_{10}-helix. The C-terminal end of the distal moiety is covalently attached to the N-terminus of the proximal ubiquitin *via* a normal peptide bond. A hydrophobic patch, consisting of Leu8, Ile44 and Val70, is shown as a stick model. Residues at the interface between the two ubiquitin moieties are also shown as a stick model. Bottom, surface representation of linear diubiquitin. The hydrophobic patch is shown in red.

stabilized by interactions between the two ubiquitin moieties. In the absence of intermoiety interactions, the relative orientations of the two moieties in free linear diubiquitin may vary in solution, and our crystal structure represents a snapshot of this dynamic process, although we do not exclude the possibility that it could be a result of crystal packing. The canonical hydrophobic patches containing Leu8, Leu44 and Val70 from each ubiquitin moiety are located on opposite surfaces relative to one another (Fig. 1). In contrast to the previously reported structure (Komander *et al.*, 2009), the crystal packing is characterized by a linear array of diubiquitin molecules, such that the canonical hydrophobic patch appears on the same side in every other moiety along the virtual linear polyubiquitin chain (Fig. 2).

3.2. Comparison with other polyubiquitin structures

The previously reported crystal structures of linear and Lys63-linked diubiquitins revealed a fully extended conformation with the same space group and similar unit-cell parameters after crystallization under the same conditions (Komander *et al.*, 2009). In this study, we obtained crystals using different crystallization conditions. The new compact conformation of linear diubiquitin also differs from other reported polyubiquitin structures containing Lys6-based (Virdee *et al.*, 2010), Lys11-based (Bremm *et al.*, 2010; Matsumoto *et al.*, 2010) and Lys48-based linkages (Cook *et al.*, 1992). Fig. 3 shows a comparison of diubiquitin structures with different linkage types. Interestingly, the positions of the canonical hydrophobic patches are different. In Lys6-linked and Lys48-linked diubiquitins one or both hydrophobic patches are involved in intermoiety interactions. In Lys11-linked, Lys63-linked and linear diubiquitin structures the hydrophobic patches are exposed to the solvent. In this study the hydrophobic surfaces of the ubiquitin moieties alternate on opposite sides of the linear diubiquitin structure (Fig. 2), unlike other structures in which the hydrophobic patches are more or less on the same side.

Table 2
Average values of *B* factors for residues in the linker region of the linear diubiquitin.

Residue	B_{avg} (Å^2)
Distal Arg72	34.2
Distal Leu73	36.9
Distal Arg74	43.5
Distal Gly75	40.7
Distal Gly76	37.6
Proximal Met1	31.1
Proximal Gln2	31.0

The crystal structures of Lys48-linked polyubiquitin chains are markedly different from other polyubiquitin chains. Lys48-linked diubiquitins and tetraubiquitins adopt compact conformations stabilized by extensive hydrophobic interactions between the canonical hydrophobic surfaces (Cook *et al.*, 1992; Phillips *et al.*, 2001; Eddins *et al.*, 2007; Trempe *et al.*, 2010); this is in agreement with NMR analyses, which show a closed conformation for Lys48-linked tetraubiquitin (Eddins *et al.*, 2007). Another NMR study, however, showed that Lys48-linked diubiquitin changes from an 'open' to a 'closed' conformation as pH levels increase, suggesting that diubiquitin chains are dynamic and flexible in solution (Varadan *et al.*, 2002). The dynamic nature of diubiquitin chains is supported by a crystal structure of Lys48-linked tetraubiquitin obtained at acidic pH in which the canonical hydrophobic patch is not buried (Cook *et al.*, 1994).

Lys6-linked diubiquitin chains have a compact conformation, with a hydrophobic interface where Ile44 of the distal ubiquitin is engaged, while Ile44 of the proximal ubiquitin is exposed to the solvent (Virdee *et al.*, 2010; Fig. 3). Recently, two different crystal structures of Lys11-linked diubiquitin have been reported (Bremm *et al.*, 2010; Matsumoto *et al.*, 2010). In one of them (PDB

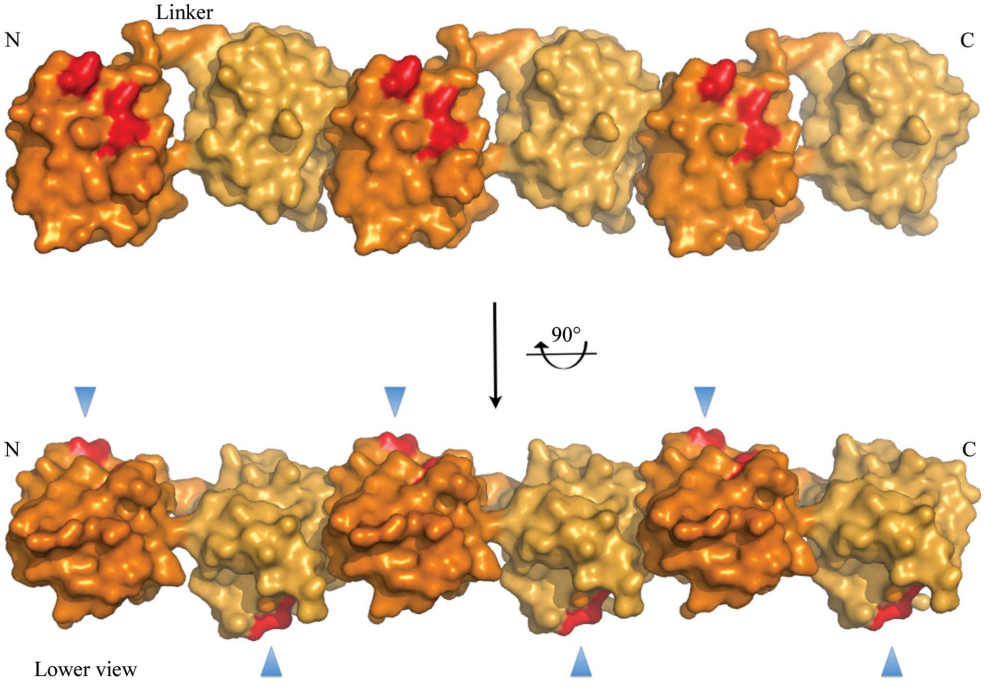

Figure 2
A surface representation of two adjacent linear diubiquitin molecules in two views related by a 90° rotation around the horizontal axis. The distal ubiquitins are denoted in darker orange, whereas the proximal moieties are shown in tan. The hydrophobic patches (Leu8, Ile44 and Val70) are shown in red and are aligned on the same side in every other moiety along the straight line of linear diubiquitin chains in the crystal. The orientation of the linear molecule is the same as in Fig. 1. The blue arrowheads represent the locations of hydrophobic patches.

entry 3nob), Leu8 and Val70 from the canonical hydrophobic patch are located at the interface between the two ubiquitin moieties, whereas Ile44 is exposed to the solvent and does not contribute to intermoiety interactions (Matsumoto *et al.*, 2010). Overall, the two hydrophobic patches merge to form a larger hydrophobic surface (Fig. 3). The second crystal structure of Lys11-linked diubiquitin (PDB entry 2xew) shares some characteristics with the linear diubiquitin reported in this study (Bremm *et al.*, 2010). When the distal ubiquitins are superimposed, the hydrophobic patches of the proximal ubiquitins are located close to each other; the Ile44 residues of the proximal ubiquitins are approximately 10 Å apart. Interestingly, superimposing the distal ubiquitins revealed that the proximal Lys11 in Lys11-linked diubiquitin is located close to the proximal Met1 in the linear diubiquitin chain.

3.3. Differences between linear and Lys63-linked polyubiquitin chains

It is worth noting that the chemical environment of the junction is different among the various polyubiquitins. In Lys63-linked polyubiquitin, the lysine residue of the proximal moiety is covalently attached to the flexible C-terminus of the distal ubiquitin. Lysine is a long and flexible residue, which, together with the C-terminal tail, gives Lys63-linked polyubiquitin a high degree of flexibility. In linear chains, however, flexibility is restrained by the methionine residue, which is shorter than and not as flexible as the Lys63 chain. Our previous study showed that the NEMO UBAN domain selectively binds linear diubiquitin chains and that the distal ubiquitin interacts *via* the canonical hydrophobic patch of the β-sheet and the C-terminal tail (Rahighi *et al.*, 2009). On the other hand, the proximal ubiquitin binds NEMO *via* polar interactions, which involve a series of residues located on the noncanonical side of the β-sheet near the N-terminus of the proximal ubiquitin. Superimposing the distal ubiquitin of free linear diubiquitin on that of the NEMO complex crystal structure demonstrates that binding to NEMO results in a conformational change in the linear diubiquitin; the C-terminus of the distal ubiquitin and the N-terminus of the proximal ubiquitin move closer to interact with NEMO (Figs. 4*a* and 4*b*). Furthermore, binding to NEMO induces a

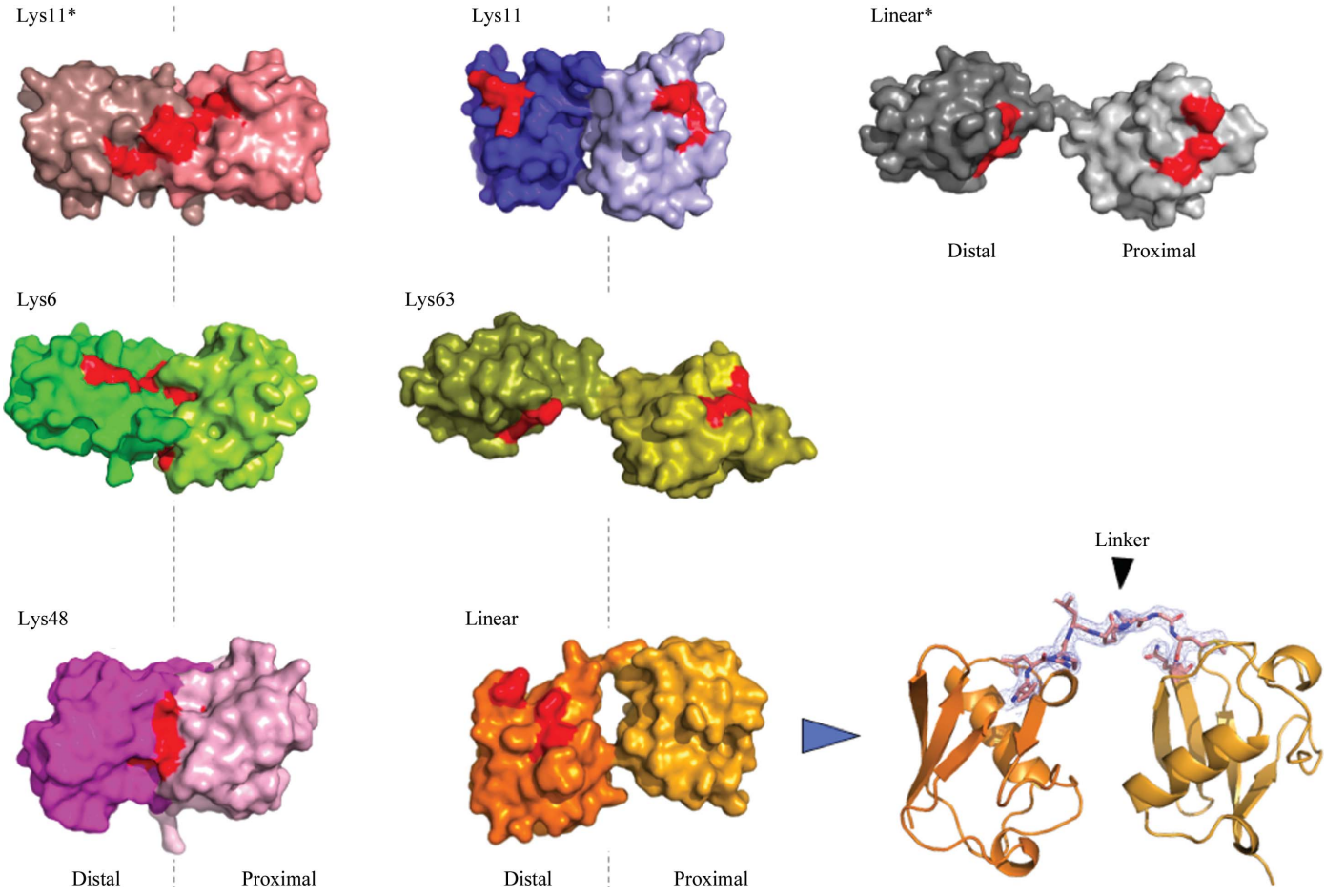

Figure 3
Comparison of crystals of Lys11-linked (PDB entry 3nob; labelled Lys11*; Matsumoto *et al.*, 2010), Lys11-linked (PDB entry 2xew; Bremm *et al.*, 2010), Lys6-linked (PDB entry 2xk5; Virdee *et al.*, 2010), Lys48-linked (PDB entry 1aar; Cook *et al.*, 1992), Lys63-linked (PDB entry 2jf5; Komander *et al.*, 2009), linear (PDB entry 2w9n; labelled linear*; Komander *et al.*, 2009) and linear diubiquitin (this study) showing electron density of the linker contoured at 1σ (lower right). The proximal ubiquitin moieties are shown in the lighter colour. The hydrophobic patches (Leu8, Ile44 and Val70) are denoted in red.

slight twist around the linker region, which causes a spatial transition of the proximal ubiquitin from the free to the bound form (Fig. 4*c*). This shift locks residues from the linker and N-terminus in position to interact with NEMO, a conformation that cannot be achieved by Lys63- or Lys48-linked diubiquitin. The previously reported extended conformation of linear diubiquitin also requires large conformational changes to bind to NEMO (Fig. 4*d*). Our new crystal structure represents one linear chain-specific conformation. The subtle differences between the diubiquitin chains affect specific binding by the UBAN domain and possibly other ubiquitin-binding domains.

A recent comparative study using NMR residual dipolar coupling revealed that among a pool of conformational diversity, ubiquitin and UBD interact *via* conformational selection and proposed the coexistence of the bound and free form of ubiquitin in solution (Lange *et al.*, 2008). In a follow-up study, Wlodarski & Zagrovic (2009) proposed that conformational selection is followed by a second step, the 'induced fit', which optimizes the orientation of the residues surrounding the binding surface, adding a second layer of specific molecular recognition, it is these local residual differences that account for the specific molecular recognition in addition to conformational selection.

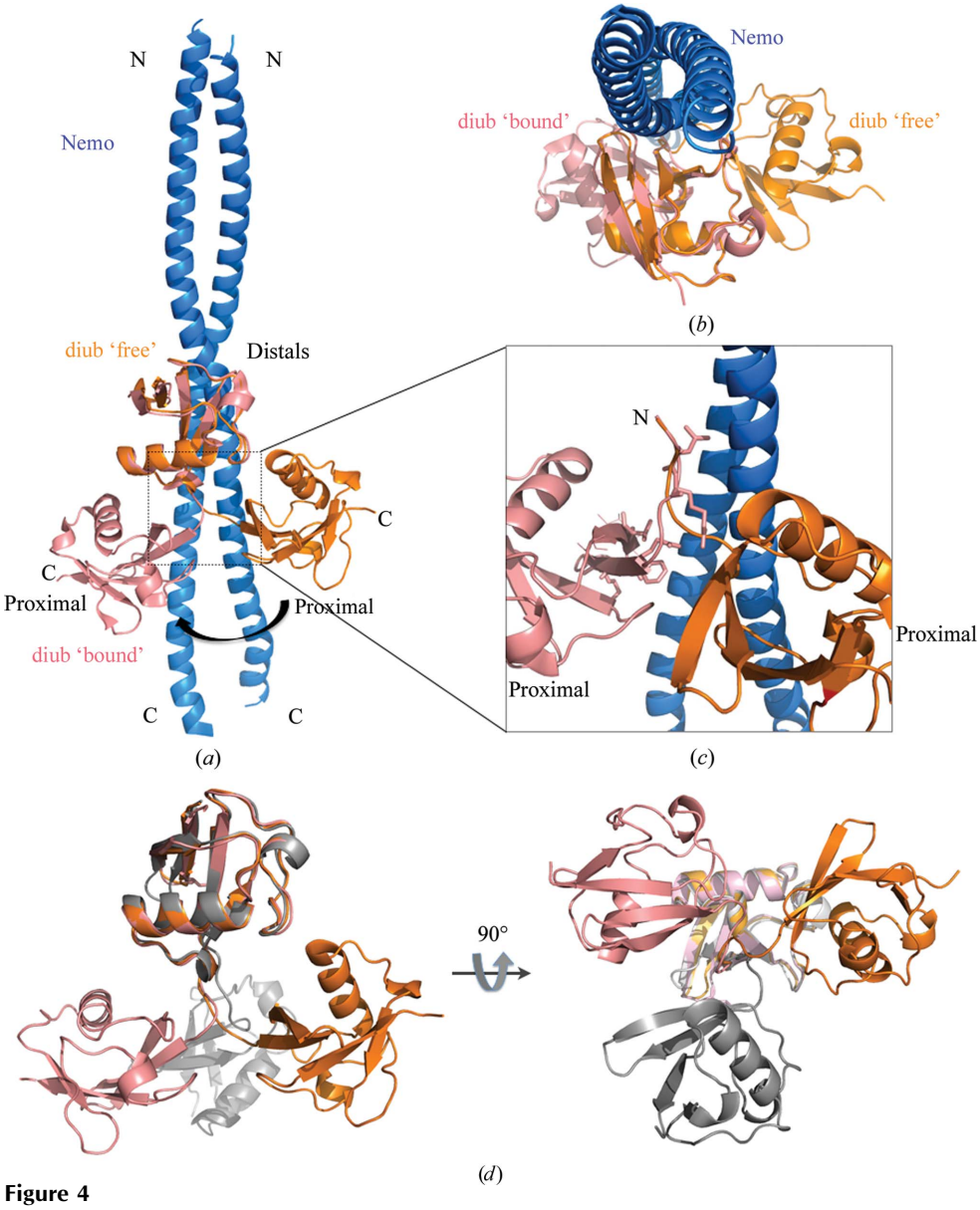

Figure 4
Superimposition of the crystal structures of distal ubiquitins from free linear diubiquitin and the NEMO–linear diubiquitin complex. (*a*) Superimposition of diubiquitin (orange) on diubiquitin (pink) complexed with the NEMO UBAN domain (blue). Binding to NEMO induces a conformational change in linear diubiquitin (indicated by the arrow), resulting in a twist in the linker region. (*b*) View orthogonal to (*a*). The distal ubiquitin interacts with NEMO *via* the hydrophobic patch, whereas the proximal ubiquitin binds *via* N-terminal residues. (*c*) The conformational change brings residues in the linker region and the N-terminus of the proximal ubiquitin into position to interact with the NEMO UBAN domain. To simplify the figure, distal ubiquitin has been removed except for the last four C-terminal residues. Side chains of diubiquitin residues interacting with NEMO are drawn as sticks. (*d*) Superposition of the linear diubiquitin chains from NEMO-bound form (pink), free forms from the current study (orange) and from Komander *et al.* (2009) (grey). The left and right panels show the same views as in (*a*) and (*b*), respectively.

4. Conclusion

The specificity of polyubiquitin signalling is dictated by the topology of ubiquitin chains, including the relative positions, orientations and other characteristics of the hydrophobic patches and the linker region. In this study, we have determined a crystal structure of linear diubiquitin that differs from the previously reported structure owing to the flexibility of the diubiquitin molecules and linker region. Upon binding the NEMO UBAN domain, linear diubiquitin in this compact conformation must undergo conformational changes to make specific interactions taking advantage of the relative orientation of the ubiquitin moieties. Our results thus suggest the need to explore polyubiquitin chains of different linkages that might exhibit subtle differences; these structural differences directly affect distinct signalling in various biological processes.

We wish to thank the beamline staff at the Photon Factory for data collection. This work was supported in part by a Grant-in-

Aid for Scientific Research and Targeted Protein Reseaerch Program from MEXT.

References

Bremm, A., Freund, S. M. & Komander, D. (2010). *Nature Struct. Mol. Biol.* **17**, 939–947.

Cook, W. J., Jeffrey, L. C., Carson, M., Chen, Z. & Pickart, C. M. (1992). *J. Biol. Chem.* **267**, 16467–16471.

Cook, W. J., Jeffrey, L. C., Kasperek, E. & Pickart, C. M. (1994). *J. Mol. Biol.* **236**, 601–609.

Datta, A. B., Hura, G. L. & Wolberger, C. (2009). *J. Mol. Biol.* **392**, 1117–1124.

Dikic, I., Wakatsuki, S. & Walters, K. J. (2009). *Nature Rev. Mol. Cell Biol.* **10**, 659–671.

Eddins, M. J., Varadan, R., Fushman, D., Pickart, C. M. & Wolberger, C. (2007). *J. Mol. Biol.* **367**, 204–211.

Emsley, P., Lohkamp, B., Scott, W. G. & Cowtan, K. (2010). *Acta Cryst.* D**66**, 486–501.

Gerlach, B. *et al.* (2011). *Nature (London)*, **471**, 591–596.

Grabbe, C., Husnjak, K. & Dikic, I. (2011). *Nature Rev. Mol. Cell Biol.* **12**, 295–307.

Haglund, K., Di Fiore, P. P. & Dikic, I. (2003). *Trends Biochem. Sci.* **28**, 598–603.

Hershko, A. & Ciechanover, A. (1998). *Annu. Rev. Biochem.* **67**, 425–479.

Hicke, L. (2001). *Nature Rev. Mol. Cell Biol.* **2**, 195–201.

Hiraki, M. *et al.* (2006). *Acta Cryst.* D**62**, 1058–1065.

Ikeda, F., Crosetto, N. & Dikic, I. (2010). *Cell*, **143**, 677–681.

Ikeda, F. & Dikic, I. (2008). *EMBO Rep.* **9**, 536–542.

Ikeda, F. *et al.* (2011). *Nature (London)*, **471**, 637–641.

Iwai, K. & Tokunaga, F. (2009). *EMBO Rep.* **10**, 706–713.

Kirisako, T., Kamei, K., Murata, S., Kato, M., Fukumoto, H., Kanie, M., Sano, S., Tokunaga, F., Tanaka, K. & Iwai, K. (2006). *EMBO J.* **25**, 4877–4887.

Komander, D., Reyes-Turcu, F., Licchesi, J. D., Odenwaelder, P., Wilkinson, K. D. & Barford, D. (2009). *EMBO Rep.* **10**, 466–473.

Lange, O. F., Lakomek, N. A., Farès, C., Schröder, G. F., Walter, K. F., Becker, S., Meiler, J., Grubmüller, H., Griesinger, C. & de Groot, B. L. (2008). *Science*, **320**, 1471–1475.

Li, W. & Ye, Y. (2008). *Cell. Mol. Life Sci.* **65**, 2397–2406.

Matsumoto, M. L., Wickliffe, K. E., Dong, K. C., Yu, C., Bosanac, I., Bustos, D., Phu, L., Kirkpatrick, D. S., Hymowitz, S. G., Rape, M., Kelley, R. F. & Dixit, V. M. (2010). *Mol. Cell*, **39**, 477–484.

Murshudov, G. N., Skubák, P., Lebedev, A. A., Pannu, N. S., Steiner, R. A., Nicholls, R. A., Winn, M. D., Long, F. & Vagin, A. A. (2011). *Acta Cryst.* D**67**, 355–367.

Otwinowski, Z. & Minor, W. (1997). *Methods Enzymol.* **276**, 307–326.

Phillips, C. L., Thrower, J., Pickart, C. M. & Hill, C. P. (2001). *Acta Cryst.* D**57**, 341–344.

Pickart, C. M. (2001). *Annu. Rev. Biochem.* **70**, 503–533.

Rahighi, S., Ikeda, F., Kawasaki, M., Akutsu, M., Suzuki, N., Kato, R., Kensche, T., Uejima, T., Bloor, S., Komander, D., Randow, F., Wakatsuki, S. & Dikic, I. (2009). *Cell*, **136**, 1098–1109.

Tokunaga, F., Nakagawa, T., Nakahara, M., Saeki, Y., Taniguchi, M., Sakata, S., Tanaka, K., Nakano, H. & Iwai, K. (2011). *Nature (London)*, **471**, 633–636.

Tokunaga, F., Sakata, S., Saeki, Y., Satomi, Y., Kirisako, T., Kamei, K., Nakagawa, T., Kato, M., Murata, S., Yamaoka, S., Yamamoto, M., Akira, S., Takao, T., Tanaka, K. & Iwai, K. (2009). *Nature Cell Biol.* **11**, 123–132.

Trempe, J.-F., Brown, N. R., Noble, M. E. M. & Endicott, J. A. (2010). *Acta Cryst.* F**66**, 994–998.

Vagin, A. & Teplyakov, A. (2010). *Acta Cryst.* D**66**, 22–25.

Varadan, R., Walker, O., Pickart, C. & Fushman, D. (2002). *J. Mol. Biol.* **324**, 637–647.

Vijay-Kumar, S., Bugg, C. E. & Cook, W. J. (1987). *J. Mol. Biol.* **194**, 531–544.

Virdee, S., Ye, Y., Nguyen, D. P., Komander, D. & Chin, J. W. (2010). *Nature Chem. Biol.* **6**, 750–757.

Winget, J. M. & Mayor, T. (2010). *Mol. Cell*, **38**, 627–635.

Winn, M. D. *et al.* (2011). *Acta Cryst.* D**67**, 235–242.

Wlodarski, T. & Zagrovic, B. (2009). *Proc. Natl Acad. Sci. USA*, **106**, 19346–19351.

Xu, P. & Peng, J. (2006). *Biochim. Biophys. Acta*, **1764**, 1940–1947.